Chicken *CDS2* isoforms presented distinct spatio-temporal expression pattern and regulated by insulin in a breed-specific manner

Yuanyuan Xu, Shuping Zhang, Yujun Guo, Linge Gao, Huaiyong Zhang, Wen Chen, and Yanqun Huang[1]

College of Animal Science, Henan Agricultural University, Hengzhou 450002, China

ABSTRACT The cytidine diphosphate diacylglycerol synthases (**CDSs**) gene encodes the cytidine diphosphate-diacylglycerol (**CDP-DAG**) synthase enzyme that catalyzes the formation of CDP-diacylglycerol from phosphatidic acid. At present, there are no reports of *CDS2* in birds. Here, we identified chicken *CDS2* transcripts by combining conventional RT-PCR amplification, 5′ rapid amplification of cDNA ends (**RACE**), and 3′ RACE, explored the spatio-temporal expression profiles of total *CDS2* and the longest transcript variant *CDS2*-4, and investigated the effect of exogenous insulin on the mRNA level of total *CDS2* via quantitative RT-PCR. Four transcripts of chicken *CDS2* (*CDS2*-1, -2, -3, and -4) were identified, which were alternatively spliced at the 3′-untranslated region (**UTR**). Both total *CDS2* and *CDS2*-4 were prominently expressed in adipose tissue, and exhibited low expression in liver and pectoralis of 49-day-old chickens. Regarding the spatio-temporal expression patterns of *CDS2* in chicken, total *CDS2* exhibited a similar temporal expression tendency with a high level in the later period of incubation (embryonic day 19 [**E19**] or 1-day-old) in the brain, liver, and pectoralis. While *CDS2*-4 presented a distinct temporal expression pattern in these tissues, *CDS2*-4 levels peaked at 21 d in the brain and pectoralis, while liver *CDS2*-4 mRNA levels were highest at the early stage of hatching (E10). Total *CDS2* ($P < 0.001$) and *CDS2*-4 ($P = 0.0090$) mRNA levels in the liver were differentially regulated throughout the development of the chicken. Total *CDS2* levels in the liver of Silky chickens were higher than that of the broiler in the basal state and after insulin stimulation. Exogenous insulin significantly down-regulated the level of total *CDS2* at 240 min in the pectoralis of Silky chickens ($P < 0.01$). In conclusion, chicken *CDS2* isoforms with variation at the 3′-UTR were identified, which was prominently expressed in adipose tissue. Total *CDS2* and *CDS2*-4 presented distinct spatio-temporal expression patterns, that is they were differentially regulated with age in brain, liver, and pectoralis. Insulin could regulate chicken *CDS2* levels in a breed- and tissue-specific manner.

Key words: chicken, *CDS2*, transcript variant, gene expression, insulin

2022 Poultry Science 101:101893
https://doi.org/10.1016/j.psj.2022.101893

INTRODUCTION

Cytidine diphosphate diacylglycerol synthases (***CDS*s**) are critical enzymes that catalyze the synthesis of cytidine diphosphate diacylglycerol (**CDP-DAG**) from phosphatidic acid to phospholipids such as phosphatidylinositol, phosphatidylglycerol, and cardiolipin (Liu et al., 2014b; Qi et al., 2016a). The gene encoding *CDS* was first cloned from *Escherichia coli* in 1985 (Icho et al., 1985), while the first eukaryotic *CDS* was cloned from *Drosophila* in 1995, which shares 31% amino acid similarity with bacterial CDS (Wu et al., 1995). *CDS* cDNA sequences were subsequently cloned from yeast (Shen et al., 1996), human (Heacock et al., 1996; Lykidis et al., 1997; Weeks et al., 1997; Halford et al., 1998), rat (Saito et al., 1997), mouse (Volta et al., 1999; Inglis-Broadgate et al., 2005), and pig (Mercade et al., 2007). All eukaryotic genomes have been shown to contain *CDS* homologs (Lykidis et al., 1997; Kong et al., 2017; Blunsom et al., 2018) and the number of *CDS* genes varies in different organisms (Blunsom and Cockcroft, 2020). There is one *CDS* gene in yeast and fly (Liu et al., 2014a), and 2 *CDS* genes (*CDS1* and *CDS2*) in vertebrates (Lykidis et al., 1997), including rat, mice, human, and zebrafish (Blunsom and Cockcroft, 2020).

The expression of mammalian *CDS2* is ubiquitous (Saito et al., 1997; Volta et al., 1999; Inglis-Broadgate et al., 2005). Recent research revealed that *CDS* is involved in numerous cellular functions. Studies from *Drosophila* highlight the importance of *CDS* (***CdsA***) in the visual photo-transduction system (Wu et al., 1995). Mutations in the eye-specific *CDS* gene in *Drosophila* resulted in a defect in photo-

Received September 1, 2021.
Accepted March 22, 2022.

[1]Corresponding author: hyanqun@aliyun.com

transduction and retinal degeneration (Wu et al., 1995). *CDS* also plays an important role in the regulation of vascular endothelial growth factor-A (**VEGFA**) signaling and angiogenesis (Zhao et al., 2019). Loss of *CDS2* has been shown to cause a defect in VEGF signaling activity and angiogenic capacity in zebrafish, primarily by decreasing the level of phosphatidylinositol 4,5-bisphosphate (**PIP2**) regeneration (Pan et al., 2012). Genetic ablation of *CDS2* switches the output of VEGFA signaling from promoting angiogenesis to inducing vessel regression and tumor inhibition (Zhao et al., 2019). Recent reports have revealed that the *CDS* gene is involved in lipid metabolism (Liu et al., 2014b; Qi et al., 2016a; Kong et al., 2017; Qi et al., 2017; Xu et al., 2019), and mammalian *CDS1* and *CDS2* regulate lipid droplets through distinct mechanisms (Xu et al., 2019). Human *CDS1* and *CDS2* can create different CDP-DAG pools; *CDS2* is selective for acyl chains at the sn-1 and sn-2 positions (D'Souza et al., 2014). The importance of CDS enzymes stems from the need for cells to maintain their phosphoinositide levels, in particular, those of PIP2 (Lykidis et al., 1997; Blunsom and Cockcroft, 2020). The translocator assembly and maintenance protein 41 (Tam41) also catalyzes the synthesis of CDP-DAG using phosphatidic acid and cytidine 5′-triphosphate as substrates, it shares no sequence or structural homology with the CDS enzyme (Liu et al., 2014a; Jiao et al., 2019). In addition, CDS is an integral membrane protein, while Tam41 is a peripheral membrane protein (Liu et al., 2014a; Blunsom et al., 2018; Jiao et al., 2019).

It was reported that about approximately 92 to 94% of human genes with multiple exons undergo alternative splicing (Wang et al., 2008). Alternative splicing is closely related to the biological processes including cell proliferation, differentiation, and development, and these splicing variants may play different roles (Qi et al., 2016b; Yang et al., 2020). Rapid Amplification of cDNA Ends (**RACE**) is an efficient way to identify alternatively spliced products if the full-length sequence or even part of a gene is known (Yeku et al., 2009).

Until now, there have been no reports of the *CDS* gene in birds. In this study, we identified chicken *CDS2* transcripts by combining 5′ and 3′-RACE and conventional Reverse Transcription PCR (**RT-PCR**), analyzed the genomic structure, chromosomal synteny, spatio-temporal expression pattern, and explored the effect of exogenous insulin on chicken *CDS2*, revealing the basic characteristics of chicken *CDS2*, the related research would lay a foundation for further identifying the function of chicken *CDS2* in the regulation of chicken development and growth. In addition, as an important model animal, the related research on chicken *CDS2* would shed a light on the function of human *CDS2* from another view.

MATERIALS AND METHODS

Sample Collection

The all procedures carried out was approved by the Animal Care and Use Committee of Henan Agricultural University (approval No. HNND20191201). Chickens and fertilized eggs were obtained from the poultry germplasm resources farm of Henan Agricultural University. The 1-day-old Arbor Acres (**AA**) broilers and Silky chickens were cage raised routinely until 49 d with free access to food and water as described previously (Ji et al., 2020). The diet was prepared based on nutritional standards for broilers recommended by the NRC (Nutrient Requirements for Poultry, 1994). The fertilized eggs from the Silky population were collected and hatched under conventional conditions.

To identify the spatio-temporal characteristics of chicken *CDS2* transcripts, brain, liver, and pectoralis tissues were collected from Silky chicken embryos at E10, E15, E19, and healthy male Silky chickens at 1-day-old (newly hatched birds, D1), D21, and D49 (n = 3 for each time point).

To investigate the effect of exogenous insulin on chicken blood glucose and *CDS2* mRNA expression, at 47 d (after 12 h fasting), healthy female AA broilers (average weight, 1.86 kg, n = 28) and female Silky fowls (average weight, 0.75 kg, n = 28) were randomly selected and subjected to an insulin tolerance test with hypodermic injection of 80 μg/kg body weight insulin (n = 20 for each breed) or equal PBS solution as the control (n = 12 for each breed) as described previously (Ji et al., 2020), and birds were given feed at 120 min. In detail, 10 birds of insulin group and 12 birds of PBS group were used to determine the blood glucose concentrations at different time point via the wing vein with a handheld glucometer (ACCU-CHEK Performa, Roche, Germany), followed by 6 birds of insulin group were sacrificed at 0, 120, and 240 min after insulin injection for sampling. The related samples were collected and snap-frozen immediately in liquid nitrogen and transfer to −80°C for RNA isolation.

RNA Extraction and First-Strand Complementary DNA Synthesis

Total RNA was extracted from tissues according to the manufacturer's instructions (RNAiso Plus, TaKaRa, Dalian, China). The quality and concentration of the extracted RNA was determined by agarose gel electrophoresis and a spectrophotometer (Thermo NanoDrop One, DE), respectively, and then the RNA for RT-PCR was reverse-transcribed using a PrimeScript RT reagent Kit with gDNA Eraser (TaKaRa) in a 20 μL reaction containing 1 μg of total RNA and random primers. The synthesized cDNA samples were stored at −20°C.

Identification of CDS2 Transcripts

CDS2 transcripts were identified by combining conventional RT-PCR amplification and 5′ and 3′ rapid amplification of cDNA ends (RACE). The primers for amplifying the *CDS2* gene were designed based on the sequence of EST CR406381.1 and the predicted chicken *CDS2* sequence (accession no. XM_417669, XM_004947552

and XM_004947553), and listed in Table S1. *CDS2* transcripts were identified from the ovary tissue /mix cDNA of Silky chickens. Specifically, *CDS2* transcripts from the ovary tissue of Silky chickens was identify using 5′ and 3′ RACE with the SMART RACE cDNA Amplification Kit (Clontech Laboratories Inc., CA) according to the manufacturer's instructions. PCR was conducted in a total volume of 50 μL, containing 2.5 μL 5′ or 3′-ready cDNA, 1.0 μL GSP1 or GSP2 primer (10 μM), 2.5 μL UPM (10 μM), and 41.5 μL Master Mix and was performed according to a touchdown PCR protocol: 5 cycles of amplification (94°C for 30 s and 72°C for 3 min) followed by five cycles of 94°C for 30 s, 70°C for 30 s, and 72°C for 3 min, and 25 cycles of 94°C for 30 s, 68°C for 30 s, and 72°C for 3 min. The amplified products for 5′- and 3′-RACE were purified and cloned into the pMD-18T vector (TaKaRa), and transformed into *E. coli* DH5α. Finally, 6 to 10 positive clones for each band were confirmed by Sanger sequencing. In addition, conventional RT-PCR were used to extend the sequence, products were electrophoresed with 1.5% agarose gel, and conducted sanger sequencing.

Conventional RT-PCR

Conventional RT-PCR was conducted to determine the tissue expression profiles of chicken *CDS2* transcripts with primers presented in Table S1. The *β-actin* was used as an internal control. PCR amplification was done in a total volume of 10 μL containing 1.0 μL cDNA, 0.25 μL of each primer (10 μM) and 5 μL 2 × M5 Taq PCR Mix (Mei5bio, Beijing, China). A thermal cycling protocol as follows was used to detect the expression of objective genes: 3 min denaturation at 95°C, followed by 35 cycles of 25 s at 94°C, 25 s at 58 to 60°C, 30 s at 72°C, and the final extension step was 72°C for 5 min, then kept at 4°C forever. Finally, 5 μL PCR products were electrophoresed with 1.5% agarose gel. No template PCR products were taken as the negative control.

Quantitative Real-Time PCR

qPCR was carried out to quantity the mRNA expression of total *CDS2* and *CDS2*-4 in samples with a CFX96 Real-Time PCR Detection Systems (Bio-Rad Laboratories, Hercules, CA using 2 × M5 HiPer Dual Real-time PCR Super Mix (SYBRgreen with anti-Taq, Mei5bio). The *β-actin* gene was used as an internal control to normalize genes' expression. The primers for qPCR (Table S1) were optimized as previously described (Bustin, 2002). PCR amplification was performed in a total volume of 10 μL containing 5 μL Real-time PCR Super Mix (SYBRgreen with anti-Taq, Mei5-bio), 1.0 μL cDNA, and 0.25 μmol/L of forward and reverse primer as follows: 95°C for 5 min, followed by 40 cycles of 95°C for 10 s, 60°C for 15 s, and 72°C for 30 s, and a final incubation at 72°C for 10 min, followed by a final 5 min extension at 72°C. Three technical replicates were performed for each sample. No template PCR amplifications for objective genes were taken as the negative control. Relative gene expression was calculated using the $2^{-\Delta\Delta Ct}$ method (Lykidis *et al.*, 1997). In addition, the data with relatively large variations were re-examined and confirmed by qPCR.

Bioinformatics Analysis

CDS2 sequence similarity was compared with the NCBI database (https://www.ncbi.nlm.nih.gov/). The genomic structure of chicken *CDS2* was analyzed with the UCSC Genome Browser (http://genome.ucsc.edu/cgi-bin/hgBlat). PhyloView in Genomicus v100.01 was used to analyze the consensus conserved genomic synteny of *CDS2* (https://www.genomicus.biologie.ens.fr/genomicus-100.01/cgi-bin/search.pl). Amino acid sequence alignment was performed using ClustalW software. A neighbor-joining phylogenetic tree was constructed based on aligned amino acid sequence using MEGA 6.0, and edited by the tree view program with a bootstrap value of 1,000.

Statistical Analysis

Data were analyzed by one-way analysis of variance using IBM SPSS Statistics 22.0 software and expressed as mean ± standard error. Multiple comparisons were conducted using the Bonferroni method. GraphPad Prism 5.0 software was used to prepare graphs. $P < 0.05$ was considered significant and $P < 0.01$ was considered extremely significant.

RESULTS

Cloning and Identification of Chicken CDS2 Splice Variants

In the NCBI database, there are three predicted transcripts of chicken *CDS2* (XM_417669, XM_004947552 and XM_004947553) with difference in the 5′ region (about 220 bp). Comparing with XM_417669, XM_004947553 had longer predicted 5′- untranslated region (UTR) and an "AGTTGC" deletion in the predicted 5′ coding region, while XM_004947552 had big difference with XM_004947553 and XM_417669 in the 5′ sequence (about 220bp). Based on EST sequence (CR406381.1) and the predicted chicken *CDS2* sequence (XM_417669, XM_004947553 and XM_004947552), four *CDS2* transcripts alternatively spliced at the 3′-UTR were cloned by combining conventional PCR amplification (LP1-LP5, Figure S1), 5′ RACE (Figure 1A), and 3′ RACE (Figure 1B) and named as *CDS2*-1 (4,643 bp, GenBank accession no. KC886604), *CDS2*-2 (4,770 bp, GenBank accession no. KC886602), *CDS2*-3 (4,893 bp, GenBank accession no. KC886601), and *CDS2*-4 (5545 bp, GenBank accession no. KC886603). The gained longest transcript *CDS2*-4 was consistent with chicken predicted *CDS2* nucleotide sequence XM_417669 and XM_004947553. Cloned

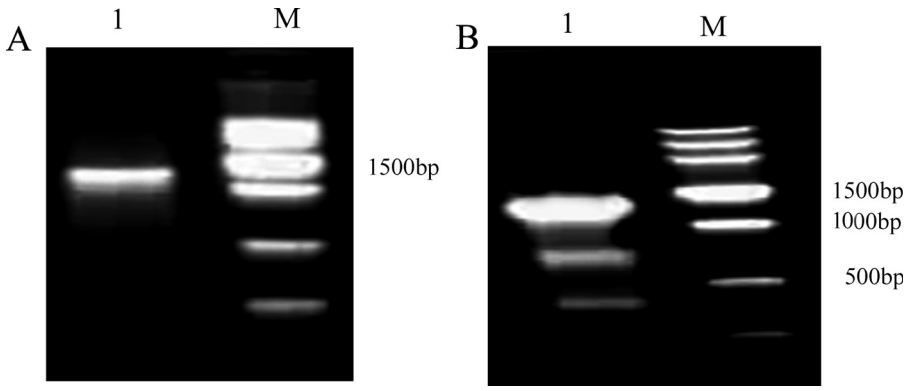

Figure 1. Gel electrophotogram of 5′ and 3′ RACE products of the *CDS2* gene. (A) 5′ RACE; and (B) 3′ RACE. 1, RACE products; M, marker.

CDS2 transcripts containing part of the 5′-UTR, 1,348 bp coding sequence (same as the predicted coding sequence of XM_417669), and a long 3′-UTR ranged from 3,265 to 4,167 bp with a polyA signal (AATAAA) and polyA tail, with differences at 4,310 to 5,210 bp compared with the longest transcript *CDS2*-4, and were predicted to encode proteins of 448 amino acids.

Chicken *CDS2* is located at chr.22, spanning approximately 23 kb of the genome (Table S2). The longest splice form (*CDS2*-4) contains 13 exons with the exon-intron boundary (Table S2) abiding by the GT-AG rule; while *CDS2*-1, *CDS2*-2, and *CDS2*-3 contain 14 exons. The exon-intron boundary of intron 13 abides by AC-AG for *CDS2*-3, GC-CA for *CDS2*-2, and CT-AG for *CDS2*-1 (http://genome.ucsc.edu/cgi-bin/hgBlat, Table S2).

Conservation of CDS2 Sequences Among Species

We investigated the sequence similarity of the coding sequence, predicted AA sequence, and the 3′-UTR of *CDS2* among species. The chicken *CDS2* coding sequence shared 96% similarity with turkey (XM_021375090.1), 94% with duck (XM_032204029.1), 81.0% with human (NM_003818.3), 81.2% with mouse (NM_138651.6), 81.1% with cattle (NM_001078046.1), 76.5% with frog (NM_001126503.1), and 78.7% with zebrafish (NM_201186.1). The deduced amino acid sequence of chicken *CDS2* shared 99.1% homology with turkey (XP_010721376.1), 97% with duck (XP_032059919.1), 91.4% with human (NP_003809.1), 93.0% with mouse (NP_619592.1), 91.0% with cattle (NP_001071514.1), 85.9% with zebrafish (NP_957480.1), and 87.7% with frog (NP_001119975.1; Figure 2A). The 3′-UTR sequence of chicken *CDS2* (KC886603) was also conserved among birds, which shares 87.7% identity with quail (XM_015883014.2), 75.3% with duck (XM_032204029.1), and 75.2% with goose (XM_013199234.1), while no identical sequences were identified in the 3′-UTR of *CDS2* between birds and mammals (data not shown).

Syntenic analysis revealed that chicken *CDS2* was located between PCNA and ARHGAP25/BMP10 on chr.22, close to the chromosomal breakage/fusion point of the mammalian/bird evolutionary event. The upstream chromosomal region of *CDS2* in birds containing the CDS2-PCNA-TMEM230-SVCT gene is homologous to chr.20 in human and chr.2 in mouse while the downstream chromosomal region containing ARHGAP25-BMP10-GKN2-GKN1 was homologous to chr.2 in human and chr.6 in mouse (Figure 3). The amino acid phylogenetic tree of CDS2 (Figure 2B) reflects the evolutionary relationship among species similar to the syntenic analysis of chromosomes (Figure 3).

Tissue Expression Profile of Chicken CDS2

We conducted RT-PCR and qPCR to investigate the tissue expression pattern of chicken *CDS2* in 49-day-old Silky chickens with AS1, CP2, and QP2 primer sets (Table S1). Primer pair AS1, spanning the alternative splicing region, can simultaneously amplify 4 splicing forms; It showed that *CDS2*-4 was predominantly expressed in all detected tissues, while the expression of isoforms *CDS2*-3, *CDS2*-1, and *CDS2*-2 was weak as detected by 3′-RACE (Figure 4).

CP2 primer set located in the coding region, whose amplification could reflect the total expression level of *CDS2* (referred to as total *CDS2*). The qPCR revealed that total *CDS2* was relatively highly expressed in adipose tissues including sebum (at the tail root), abdominal fat, and neck fat, followed by heart and leg muscle, and weakly expressed in the liver and pectoralis ($P = 0.0528$, n = 3, Figure 5A).

QP2 primer set located in the specific region of the longest transcript *CDS2*-4, it could specifically detect the expression of *CDS2*-4 variant. The qPCR revealed that *CDS2*-4 had a similar expression change pattern as total *CDS2* overall. Whereas compared with the tissue expression pattern of total *CDS2* detected with the CP2 primer set ($P = 0.0528$, n = 3, Figure 5A), the level of *CDS2*-4 showed greater tissue fluctuation ($P < 0.0001$, n = 3, Figure 5B). *CDS2*-4 exhibited similar mRNA levels in heart and adipose tissues including sebum, abdominal fat, and neck fat. *CDS2*-4 level in abdominal fat was significantly higher than that in other tissues ($P < 0.01$). The *CDS2*-4 level in adipose tissues was approximately

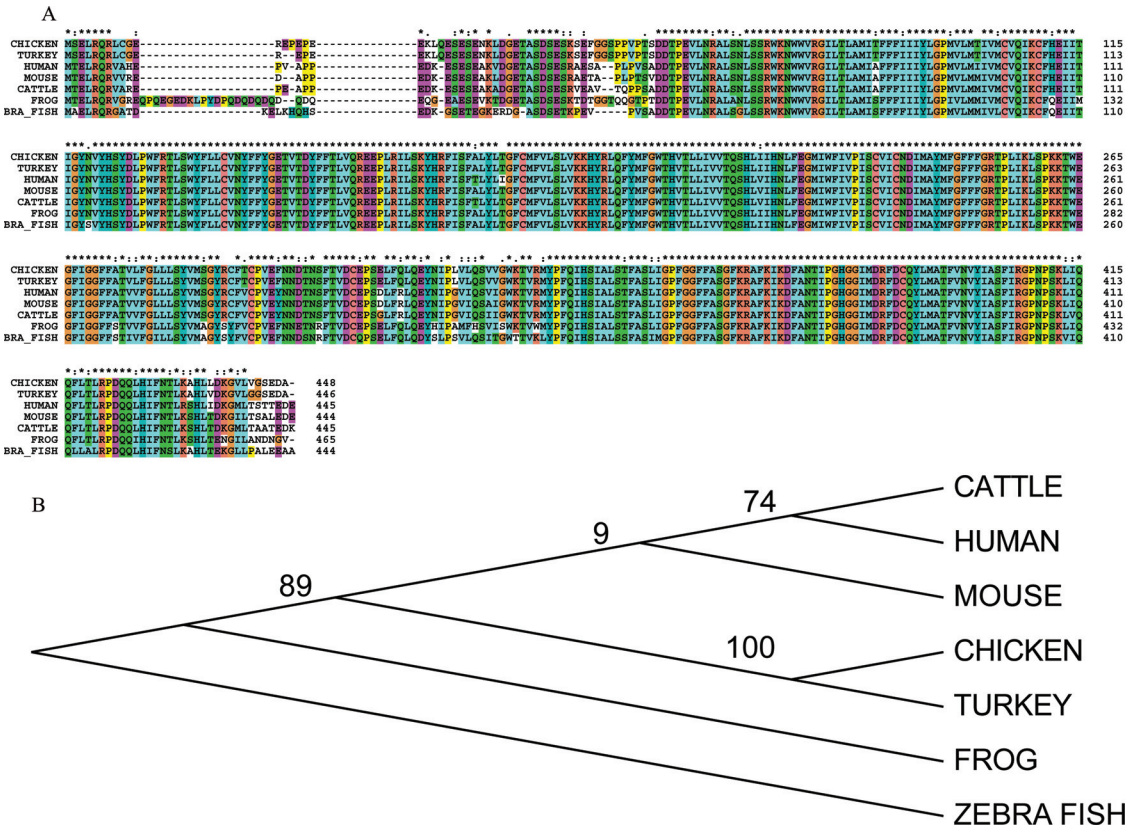

Figure 2. Amino acid comparison and phylogenetic analysis of *CDS2* gene. (A) Amino acid comparison of the *CDS2* gene among species, where highly conservative bases among species were marked with *. (B) Phylogenetic analysis of *CDS2* amino acid sequences. The distance scale was presented. The tree was constructed with aligned amino acid sequences by the neighbor-joining method.

4-fold that in the testis and 120-fold that in the liver (Figure 5B).

The Spatio-Temporal Expression Patterns of Total CDS2 and CDS2-4

We further investigated the spatio-temporal expression patterns of total *CDS2* (with the CP2 primer set) and *CDS2*-4 (with the QP2 primer set) by qPCR (n = 3). One-way ANOVA was used to analyze the effect of age and tissue on the expression of total *CDS2* and *CDS2*-4 separately. Total *CDS2* exhibited similar temporal expression patterns (Figure 6A) in the brain ($P = 0.1623$), liver ($P < 0.0001$), and pectoralis ($P = 0.1712$). The total *CDS2* mRNA level was the highest in the later stage of embryogenesis (embryonic day 19 [E19]/ one-day-old [D1]), and the E19 level in the liver was significantly higher than that of the other time points ($P < 0.05$). In addition, the relative expression of total *CDS2* in the brain was significantly ($P < 0.05$) higher than that in the liver (9-fold) and pectoralis (3-fold) at 49 d (Figure 6A).

Unlike total *CDS2*, the mRNA level of the *CDS2*-4 variant presented a distinct temporal change in pattern in the brain, liver, and pectoralis (n = 3, Figure 6B).

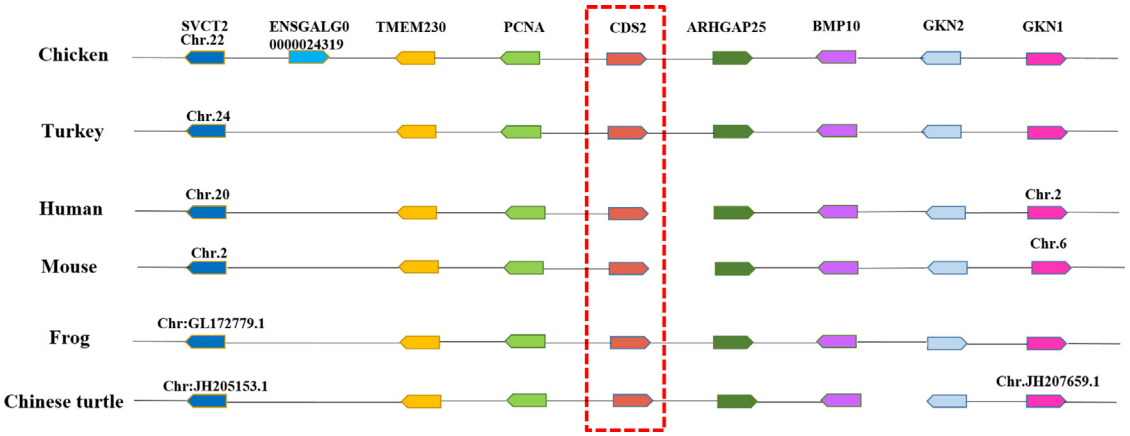

Figure 3. Gene arrangement of the genomic region encompassing *CDS2*. Boxes in the same column with the same color represent homologous genes in the corresponding species. Arrows represent the transcription direction of genes.

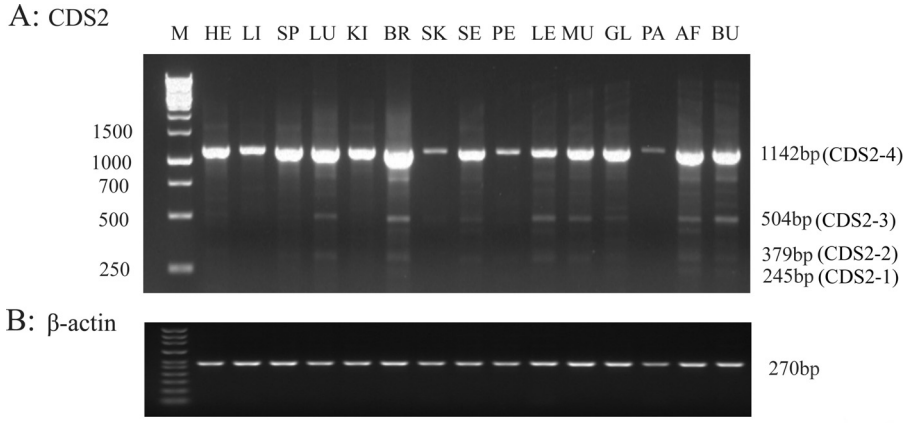

Figure 4. Tissue expression pattern of *CDS2* detected by RT-PCR with AS1 primer sets. (A) AS1 PCR products; (B) the *β*-actin gene was used as an internal control. Abbreviations: AF, abdominal fat; BU, bursa of Fabricius; BR, brain; GL, glandular stomach; HE, heart; LI, liver; LE, leg muscle; LU, lung; KI, kidney; M, DNA marker; MU, muscular stomach; PE, pectoralis; PA, pancreas; SE, sebum; SK, skin; SP, spleen.

CDS2-4 levels peaked at 21 d in the brain ($P = 0.1336$) and pectoralis ($P = 0.0104$). The level of *CDS2*-4 in the pectoralis at 21 d was significantly higher than that at the other ages tested, with the exception of 1 d ($P < 0.05$); whereas hepatic *CDS2*-4 levels presented a decreasing trend with development, with highest levels at the early stage of hatching (E10), a weak decrease during embryogenesis (E14−D1), and a clear decrease with age after hatching (D21 and D49, $P = 0.009$). Hepatic *CDS2*-4 levels at E10 were significantly higher than that at 21 d ($P < 0.05$) and 49 d ($P < 0.01$; Figure 6B). In addition, the brain had the highest level of *CDS2*-4 at all time-points among the three tissues; brain *CDS2*-4 level at 21 d was significantly higher than that in the liver and pectoralis ($P < 0.01$, Figure 6B).

Effect of Exogenous Insulin on Chicken CDS2 Expression

Exogenous insulin resulted to the rapid drop of blood glucose (until 120 min) in both Silky chickens and broilers, and Silky chickens presented a more rapid recovery of blood glucose than broilers after 120 min (Figures 7A and 7B). Exogenous insulin weakly upregulated the mRNA level of total *CDS2* at 240 min in the livers of broilers ($P = 0.078$, Figure 7C); and it downregulated the expression of total *CDS2* in the pectoralis of Silky fowl ($P = 0.003$, n = 5−6, Figure 7F), where the total *CDS2* level at 240 min was significantly lower than that at 0 and 120 min (Figure 7F). The mRNA level of total *CDS2* in the liver of Silky chickens was higher than that of broilers at the basal state and after insulin stimulation ($P < 0.05$, n = 5−6, Figure 7G); Whereas the total CDS2 level in the pectoralis of Silky chickens was lower than that of broiler chickens at 240 min after insulin injection ($P < 0.05$, n = 5−6, Figure 7H).

DISCUSSION

RACE technique is an efficient method for identifying the alternative splice variants of genes. In the present study, four isoforms alternatively spliced at the 3′-UTR

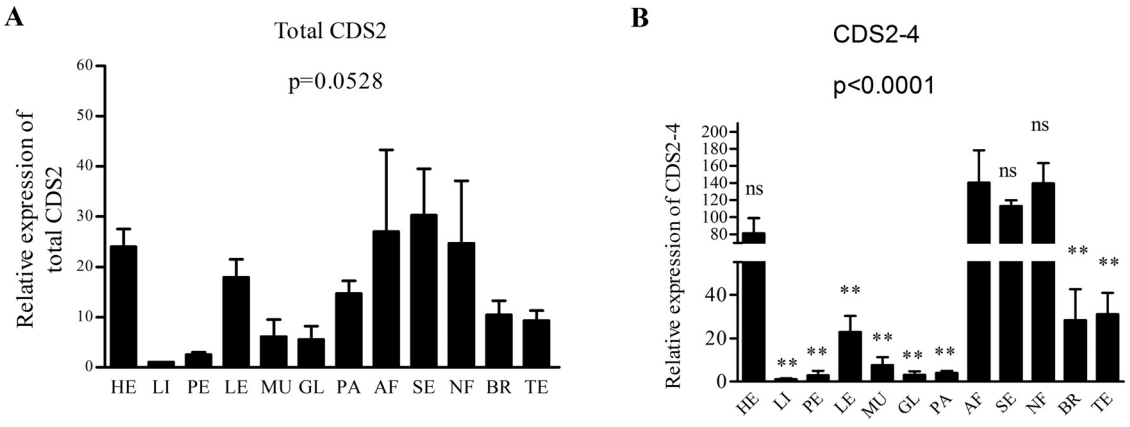

Figure 5. Tissue expression profile of chicken total *CDS2* and *CDS-4* detected by qPCR. (A)Total *CDS2*; (B) *CDS2-4*. The *β-actin* gene was used as an internal control. Data were analyzed by one-way analysis of variance and expressed as mean ± standard error. Data were analyzed by one-way analysis of variance and expressed as mean ± standard error; pair comparison was conducted using the Bonferroni method with AF as a control. **, $P < 0.01$; ns, $P > 0.05$. n = 3. Three technical replicates were performed for each sample. Abbreviations: AF, abdominal fat; BR, brain; BU, bursa of Fabricius; CA, cartilage; GL, glandular stomach; HE, heart; LE, leg muscle; LI, liver; LU, lung; KI, kidney; M, DNA marker (DL 700); MU, muscular stomach; NE, negative control; NE, neck fat; PA, pancreas; PE, pectoralis; OV, ovary; SK, skin; SE, sebum; SP, spleen; TE, testis.

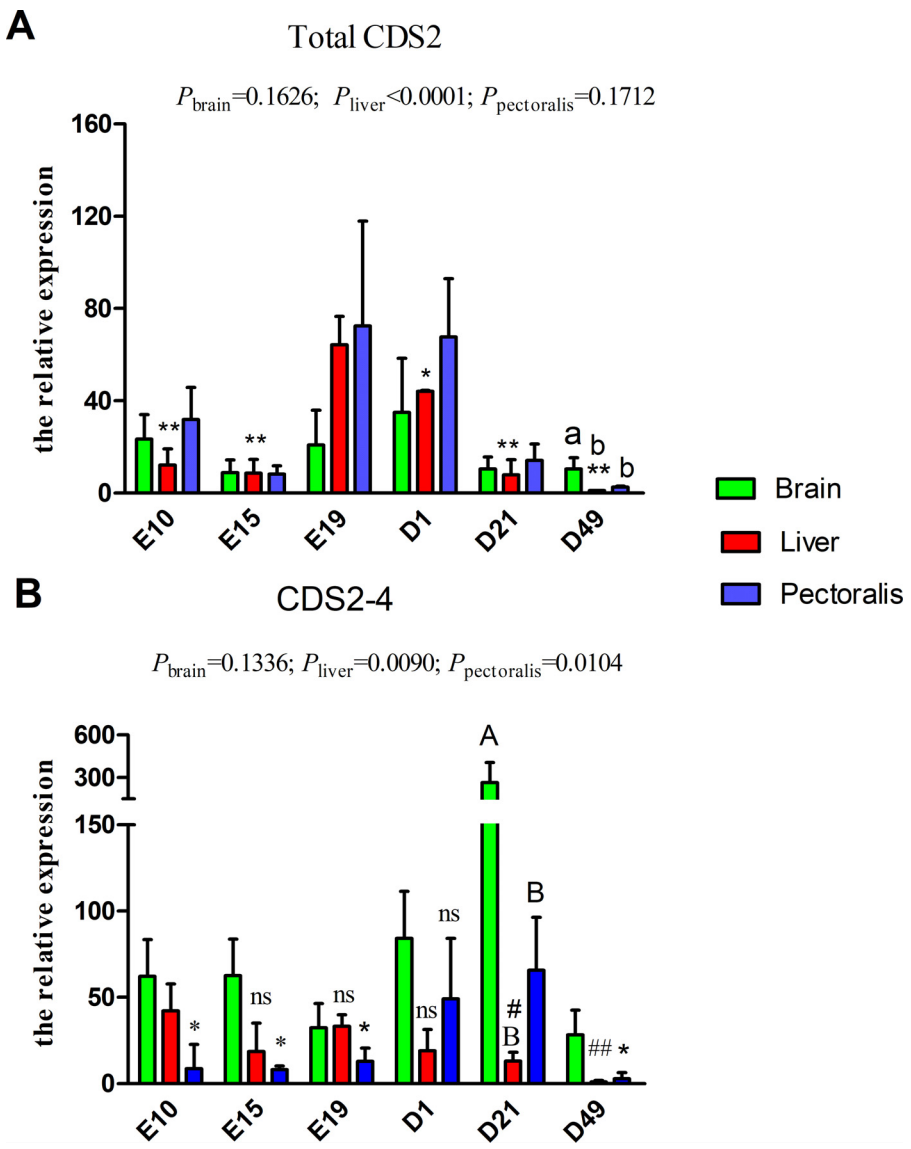

Figure 6. Spatio-temporal expression pattern of total *CDS2* and *CDS2*-4. Data were analyzed by one-way analysis of variance and expressed as mean ± standard error. Pairwise comparison was conducted using the Bonferroni method in tissues with $P < 0.05$, where the time-point with the highest value was taken as a control. * and #, $P < 0.05$; ** and ##, $P < 0.01$; ns, $P > 0.05$. Among tissues in certain time-point, different lowercase letters indicate $P < 0.05$; different uppercase letters indicate $P < 0.01$, and no symbol indicates $P > 0.05$. (A) Total *CDS2*, with E19 as a control in the liver. B. *CDS2*-4, with E10 as a control in the liver, and D21 as a control in the pectoralis. n = 3. Three technical replicates were performed for each sample.

were identified from birds' *CDS2*. It is well known that different isoforms of a single gene function differently. Transcripts expressed in low level may have important function too, which could be turned up when they are required (Pope and Medzhitov, 2018). *CDS2-4* isoform and total *CDS2* showed distinct spatio-temporal expression patterns, which suggested that the other *CDS2* isoforms (isoform 1−3) detected to be expressed in low level here should present dynamic expression in different tissues and development stages, and each isoform may function in its own manner. 3′-UTRs are major players in gene regulation that enable local function (Ciolli Mattioli et al., 2019), compartmentalization, and cooperativity (Mayr, 2017). Birds and mammals share high sequence similarity for the deduced *CDS2* proteins, while possessing their own conservative 3′-UTR, suggesting that the 3′-UTR of *CDS2* may play an important role in regulating the phenotypic diversity of higher organisms (Mayr, 2017). The average length of 3′-UTRs in human are 1,278 nt (Zhao et al., 2011); *CDS2* exhibited a long 3′-UTR both in mammals (9,000 nt in human) and birds (5,210 nt in chicken), suggesting there may be an abundance of regulatory elements in the 3′-UTR of *CDS2*. The shortening/lengthening of the 3′-UTR may result in a change in miRNA binding sites (Yuan et al., 2019). Further works are needed to identify the separate function of these isoforms and the interaction between miRNAs and chicken *CDS2*.

Here, we observed that chicken *CDS2* was predominantly expressed in multiple adipose tissues, which provide direct evidence for the function of *CDS2* in birds' lipid metabolism. *CDS* genes in mammals have been linked with lipid metabolism (Liu et al., 2014b; Qi et al., 2016a, 2017; Kong et al., 2017; Xu et al., 2019), with a

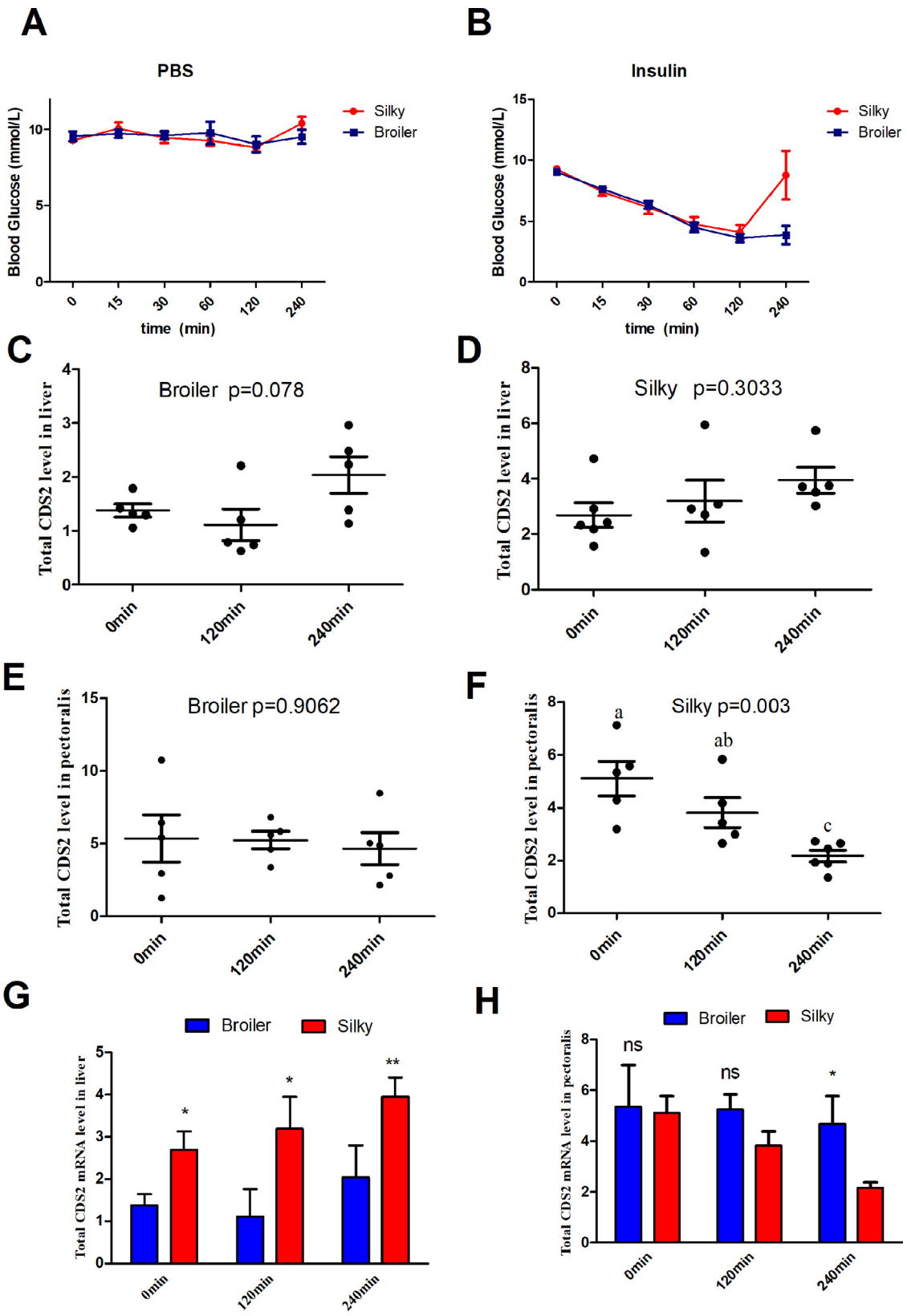

Figure 7. Effect of insulin on blood glucose and total *CDS2* mRNA levels. (A) Blood glucose in PBS control. (B) Blood glucose after insulin treatment (80 μg/kg body weight). (C) Total *CDS2* in liver of AA broilers. (D) Total *CDS2* in liver of Silky chickens. (E) Total *CDS2* in pectoralis of broilers. (F) Total *CDS2* in pectoralis of Silky chickens; G. Total *CDS2* in liver. H. total *CDS2* in pectoralis. C−F, different letters indicate $P < 0.05$, no letter or same letter indicates $P > 0.05$. In G and H, data were only compared between two breeds at the same time-point. *, $P < 0.05$; ns, $P > 0.05$. Data were analyzed by one-way analysis of variance and presented as mean ± standard error. All detected samples were included. n = 5−6. Three technical replicates were performed for each sample.

stronger effect on phosphatidic acid levels. *CDS2* deficiency (while not *CDS1*) could impair the maturation of initial lipid droplets in cultured mammalian cells (Xu et al., 2019). A transcriptome profile revealed that *CDS2* was differentially expressed in adipose tissues of fat- and short-tailed Chinese sheep (Wang et al., 2014).

Livers in birds play a central role in lipid metabolism, serving as the center for lipoprotein uptake, formation, and export to the circulation (Arvind et al., 2000; Alshamy et al., 2019), while adipose tissue functions primarily as a storage tissue (Na et al., 2018). In this study, the level of *CDS2* was low in AA chicken livers at 49 d, but where mRNA levels of *CDS2* showed dramatic temporal changes. Zhao et al. reported that hepatic triglyceride levels increased during embryonic development (Gomez and Rodriguez, 1987; Zhao et al., 2007). While post-hatching, the liver lipid content correlated negatively with broiler age; it was the highest on the first day then decreased sharply at d 7 (Noble and Ogunyemi, 1989; Alshamy et al., 2019). Here, the exhibited dynamic change pattern of total *CDS2* matched well with that of hepatic lipids during development and growth of birds, which implied that *CDS2* may participate in the regulation of hepatic lipid metabolism. In addition, total *CDS2* and *CDS2-4* present distinct temporal change feature, which indicated different *CDS2* transcripts in birds may function in a different way.

Here, we found that total *CDS2* levels in livers of Silky chickens were twice that of broilers at 47 d. Meanwhile, it has been reported that the serum lipid level (total cholesterol and triglyceride) of Silky chickens was higher than that of broilers (Ji et al., 2020), which also suggested that hepatic *CDS2* contribute to the bird's lipid metabolism. In addition, the previous data from our group found that a 30% energy restriction in broiler chickens significantly reduced the abdominal fat ratio and subcutaneous fat thickness (Chen et al., 2012), and downregulated an unknown differentially expressed fragment C7-2 (mapped to chicken EST CR406381.1; Wang et al., 2012) in broiler's liver tissue. With the update of the chicken genomic database in NCBI, this fragment has now been mapped to the 3′-UTR of chicken *CDS2* (XM_004947553, XM_417669, and XM_004947552). The downregulation of *CDS2* in chicken liver by energy restriction suggested the association of chicken *CDS2* with fat metabolism.

CDS2 was reported to be prominently expressed in brain of murine (Yue et al., 2014) and human (Fagerberg et al., 2014), here we also observed the main transcript *CDS2*-4 in birds highly expressed in the brain throughout the embryonic development and growth stage (comparing with liver and pectoralis tissues), which suggested the conservative function of *CDS2* in brain among species. The structure and function of brain also depend on intercellular exchange and de novo synthesis of lipids. Cell communication in the brain involves constant lipid exchange through lipoproteins, microvesicles, and non-esterified fatty acids (Loving and Bruce, 2020; Chausse et al., 2021).

CDS2 in *Drosophila* has been linked with insulin pathway (Liu et al., 2014b). Here we further study the insulin sensitivity of birds' *CDS2*. Silky chickens showed greater rise latitude of blood glucose than broilers at 240 min after insulin stimulation. Skeletal muscles have been considered to be a major regulator of systemic glucose homeostasis (Honka et al., 2018). In the current study, exogenous insulin significantly downregulated the level of total *CDS2* at 240 min in the pectoralis of Silky chickens, which means the birds' *CDS2* response to exogenous insulin in a breed- and tissue-specific manner. The downregulation of *CDS2* in the pectoralis of Silky may contribute to the more rapid blood glucose recovery at 240 min after insulin injection through positively downregulating the PI3K activity in the insulin pathway (Liu et al., 2014b).

Overall, chicken *CDS2* were alternatively spliced at 3′-UTR, which prominently expressed in adipose tissues and exhibited distinct spatio-temporal expression patterns during chicken development and growth. Total *CDS2* mRNA level in the liver of Silky chickens was twice of that in broilers. Total *CDS2* in pectoralis was insulin sensitive, which were significantly changed by insulin in a breed- and tissue-specific manner. Nevertheless, limited to the experiment design, monosexual birds, and limited samples were used in this study, so the impact of these factors on the findings/conclusions we made from these experiments need to be considered.

CONCLUSIONS

In summary, 4 alternatively spliced forms of *CDS2* with variations at the 3′-UTR were identified in chicken, and the longest form, *CDS2*-4, was the main transcript. Both total *CDS2* and *CDS2*-4 were extensively expressed in all detected tissues, and predominantly present in adipose tissues including sebum, abdominal fat, and neck fat. Furthermore, total *CDS2* and *CDS2*-4 presented distinct spatio-temporal expression patterns in the brain, liver, and pectoralis during chicken development and growth. Total hepatic *CDS2* and *CDS2*-4 were dramatically regulated with age in a distinctly different manner. Total *CDS2* in the liver of Silky chickens was significantly higher than that of broilers at the basal state and after insulin stimulation. Total *CDS2* mRNA level was changed by insulin in a breed- and tissue-specific manner, which was significantly downregulated at 240 min after exogenous insulin stimulation in the pectoralis of Silky chickens.

ACKNOWLEDGMENTS

This research was supported by the National Natural Science Foundation of China (32072748).

DISCLOSURES

The authors declare that they have no competing interests.

SUPPLEMENTARY MATERIALS

Supplementary material associated with this article can be found in the online version at doi:10.1016/j.psj.2022.101893.

REFERENCES

Alshamy, Z., K. C. Richardson, G. Harash, H. Hünigen, I. Röhe, H. M. Hafez, J. Plendl, and S. Al Masri. 2019. Structure and age-dependent growth of the chicken liver together with liver fat quantification: a comparison between a dual-purpose and a broiler chicken line. PLoS One 14:e0226903.

Arvind, A., S. A. Osganian, D. E. Cohen, and K. E. Corey. 2000. Lipid and Lipoprotein Metabolism in Liver Disease in Endotext. K. R. Feingold, B. Anawalt, A. Boyce, G. Chrousos, W. W. de Herder, K. Dhatariya, K. Dungan, A. Grossman, J. M. Hershman, J. Hofland, S. Kalra, G. Kaltsas, C. Koch, P. Kopp, M. Korbonits, C. S. Kovacs, W. Kuohung, B. Laferrère, E. A. McGee, R. McLachlan, J. E. Morley, M. New, J. Purnell, R. Sahay, F. Singer, C. A. Stratakis, D. L. Trence, and D. P. Wilson eds. MDText.com, Inc. Copyright © 2000-2021, MDText.com, Inc., South Dartmouth, MA.

Blunsom, N. J., and S. Cockcroft. 2020. CDP-diacylglycerol synthases (CDS): gateway to phosphatidylinositol and cardiolipin synthesis. Front. Cell Dev. Biol. 8:63.

Blunsom, N. J., E. Gomez-Espinosa, T. G. Ashlin, and S. Cockcroft. 2018. Mitochondrial CDP-diacylglycerol synthase activity is due to the peripheral protein, TAMM41 and not due to the integral membrane protein, CDP-diacylglycerol synthase 1. BBA-Mol. Cell Biol. L 1863:284–298.

Bustin, S. 2002. Quantification of mRNA using real-time reverse transcription PCR (RT-PCR): trends and problems. J. Mol. Endocrinol. 29:23–39.

Chausse, B., P. A. Kakimoto, and O. Kann. 2021. Microglia and lipids: how metabolism controls brain innate immunity. Semin. Cell Dev. Biol. 112:137–144.

Chen, W., Y. M. Guo, Y. Q. Huang, Y. H. Shi, C. X. Zhang, and J. W. Wang. 2012. Effect of energy restriction on growth, slaughter performance, serum biochemical parameters and Lpin2/WDTC1 mRNA expression of broilers in the later phase. J. Poult. Sci. 49:12–19.

Ciolli Mattioli, C., A. Rom, V. Franke, K. Imami, G. Arrey, M. Terne, A. Woehler, A. Akalin, I. Ulitsky, and M. Chekulaeva. 2019. Alternative 3′ UTRs direct localization of functionally diverse protein isoforms in neuronal compartments. Nucleic Acids Res 47:2560–2573.

D'Souza, K., Y. J. Kim, T. Balla, and R. M. Epand. 2014. Distinct properties of the two isoforms of CDP-diacylglycerol synthase. Biochemistry 53:7358–7367.

Fagerberg, L., B. M. Hallström, P. Oksvold, C. Kampf, D. Djureinovic, J. Odeberg, M. Habuka, S. Tahmasebpoor, A. Danielsson, K. Edlund, A. Asplund, E. Sjöstedt, E. Lundberg, C. A.-K. Szigyarto, M. Skogs, J. O. Takanen, H. Berling, H. Tegel, J. Mulder, P. Nilsson, J. M. Schwenk, C. Lindskog, F. Danielsson, A. Mardinoglu, A. Sivertsson, K. von Feilitzen, M. Forsberg, M. Zwahlen, I. Olsson, S. Navani, M. Huss, J. Nielsen, F. Ponten, and M. Uhlén. 2014. Analysis of the human tissue-specific expression by genome-wide integration of transcriptomics and antibody-based proteomics. Mol. Cell. Proteomics: MCP 13:397–406.

Gomez, M. A., and F. C. Rodriguez. 1987. A study of the hepatic lipids during chick embryo development effect of triiodothyronine. Exp. Clin. Endocrinol. Diabetes 90:249–252.

Halford, S., K. S. Dulai, S. C. Daw, J. Fitzgibbon, and D. M. Hunt. 1998. Isolation and chromosomal localization of two human CDP-diacylglycerol synthase (CDS) genes. Genomics 54:140–144.

Heacock, A. M., M. D. Uhler, and B. W. Agranoff. 1996. Cloning of CDP-diacylglycerol synthase from a human neuronal cell line. J. Neurochem. 67:2200–2203.

Honka, M. J., A. Latva-Rasku, M. Bucci, K. A. Virtanen, and P. Nuutila. 2018. Insulin stimulated glucose uptake in skeletal muscle, adipose tissue and liver: a positron emission tomography study. Eur. J. Endocrinol. 178:523–531.

Icho, T., C. P. Sparrow, and C. R. Raetz. 1985. Molecular cloning and sequencing of the gene for CDP-diglyceride synthetase of Escherichia coli. J. Biol. Chem. 260:12078–12083.

Inglis-Broadgate, S. L., L. Ocaka, R. Banerjee, M. Gaasenbeek, J. P. Chapple, M. E. Cheetham, B. J. Clark, D. M. Hunt, and S. Halford. 2005. Isolation and characterization of murine Cds (CDP-diacylglycerol synthase) 1 and 2. Gene 356:19–31.

Ji, J. F., Y. F. Tao, X. L. Zhang, J. J. Pan, X. H. ZHu, H. J. Wang, P. F. Du, Y. Zhu, Y. Q. Huang, and W. Chen. 2020. Dynamic changes of blood glucose, serum biochemical parameters and gene expression in response to exogenous insulin in Arbor Acres broilers and Silky fowls. Sci. Rep. 10:6697.

Jiao, H., Y. Yin, and Z. Liu. 2019. Structures of the mitochondrial CDP-DAG synthase tam41 suggest a potential lipid substrate pathway from membrane to the active site. Structure 27 1258-1269.e1254.

Kong, P., C. M. Ufermann, D. L. M. Zimmermann, Q. Yin, X. Suo, J. B. Helms, J. F. Brouwers, and N. Gupta. 2017. Two phylogenetically and compartmentally distinct CDP-diacylglycerol synthases cooperate for lipid biogenesis in Toxoplasma gondii. J. Biol. Chem. 292:7145–7159.

Liu, X., Y. Yin, J. Wu, and Z. Liu. 2014a. Structure and mechanism of an intramembrane liponucleotide synthetase central for phospholipid biosynthesis. Nat. Commun. 5:4244.

Liu, Y., W. Wang, G. Shui, and X. Huang. 2014b. CDP-diacylglycerol synthetase coordinates cell growth and fat storage through phosphatidylinositol metabolism and the insulin pathway. PLoS Genet 10:e1004172.

Loving, B. A., and K. D. Bruce. 2020. Lipid and lipoprotein metabolism in microglia. Front. Physiol. 11:393.

Lykidis, A., P. D. Jackson, C. O. Rock, and S. Jackowski. 1997. The role of CDP-diacylglycerol synthetase and phosphatidylinositol synthase activity levels in the regulation of cellular phosphatidylinositol content. J. Biol. Chem. 272:33402–33409.

Mayr, C. 2017. Regulation by 3 -Untranslated Regions. Annu. Rev. Genet. 51:171–194.

Mercade, A., A. Sanchez, and J. Folch. 2007. Characterization and physical mapping of the porcine CDS1 and CDS2 genes. Anim. Biotechnol. 18:23–35.

Na, W., Y. Y. Wu, P. F. Gong, C. Y. Wu, B. H. Cheng, Y. X. Wang, N. Wang, Z. Q. Du, and H. Li. 2018. Embryonic transcriptome and proteome analyses on hepatic lipid metabolism in chickens divergently selected for abdominal fat content. BMC Genomics 19:384.

Noble, R. C., and D. Ogunyemi. 1989. Lipid changes in the residual yolk and liver of the chick immediately after hatching. Biol. Neonate 56:228–236.

Pan, W., V. N. Pham, A. N. Stratman, D. Castranova, M. Kamei, K. R. Kidd, B. D. Lo, K. M. Shaw, J. Torres-Vazquez, C. M. Mikelis, J. S. Gutkind, G. E. Davis, and B. M. Weinstein. 2012. CDP-diacylglycerol synthetase-controlled phosphoinositide availability limits VEGFA signaling and vascular morphogenesis. Blood 120:489–498.

Pope, S. D., and R. Medzhitov. 2018. Emerging principles of gene expression programs and their regulation. Mol. Cell 71:389–397.

Qi, Y., T. Kapterian, X. Du, Q. Ma, W. Fei, Y. Zhang, X. Huang, I. Dawes, and H. Yang. 2016a. CDP-diacylglycerol synthases regulate the growth of lipid droplets and adipocyte development. J. Lipid Res. 57:767–780.

Qi, Y., L. Sun, and H. Yang. 2017. Lipid droplet growth and adipocyte development: mechanistically distinct processes connected by phospholipids. BBA-Mol. Cell Biol. L 1862:1273–1283.

Qi, Y., J. Yu, W. Han, X. Fan, H. Qian, H. Wei, Y. H. Tsai, J. Zhao, W. Zhang, Q. Liu, S. Meng, Y. Wang, and Z. Wang. 2016b. A splicing isoform of TEAD4 attenuates the Hippo-YAP signalling to inhibit tumour proliferation. Nat. Commun. 7 ncomms11840.

Saito, S., K. Goto, A. Tonosaki, and H. Kondo. 1997. Gene cloning and characterization of CDP-diacylglycerol synthase from rat brain. J. Biol. Chem. 272:9503.

Shen, H., P. N. Heacock, C. J. Clancey, and W. Dowhan. 1996. The CDS1 gene encoding CDP-diacylglycerol synthase in Saccharomyces cerevisiae is essential for cell growth. J. Biol. Chem. 271:789–795.

Volta, M., A. Bulfone, C. Gattuso, E. Rossi, M. Mariani, G. G. Consalez, O. Zuffardi, A. Ballabio, S. Banfi, and

B. Franco. 1999. Identification and characterization of CDS2, a mammalian homolog of the Drosophila CDP-diacylglycerol synthase gene. Genomics 55:68–77.

Wang, E. T., R. Sandberg, S. Luo, I. Khrebtukova, L. Zhang, C. Mayr, S. F. Kingsmore, G. P. Schroth, and C. B. Burge. 2008. Alternative isoform regulation in human tissue transcriptomes. Nature 456:470–476.

Wang, J., W. Chen, X. Kang, Y. Huang, Y. Tian, and Y. Wang. 2012. Identification of differentially expressed genes induced by energy restriction using annealing control primer system from the liver and adipose tissues of broilers. Poult. Sci. 91:972–978.

Wang, X., G. Zhou, X. Xu, R. Geng, J. Zhou, Y. Yang, Z. Yang, and Y. Chen. 2014. Transcriptome profile analysis of adipose tissues from fat and short-tailed sheep. Gene 549:252–257.

Weeks, R., W. Dowhan, H. Shen, N. Balantac, B. Meengs, E. Nudelman, and D. W. Leung. 1997. Isolation and expression of an isoform of human CDP-diacylglycerol synthase cDNA. DNA Cell Biol 16:281–289.

Wu, L., B. Niemeyer, N. Colley, M. Socolich, and C. S. Zuker. 1995. Regulation of PLC-mediated signalling in vivo by CDP-diacylglycerol synthase. Nature 373:216–222.

Xu, Y., H. Y. Mak, I. Lukmantara, Y. E. Li, K. L. Hoehn, X. Huang, X. Du, and H. Yang. 2019. CDP-DAG synthase 1 and 2 regulate lipid droplet growth through distinct mechanisms. J. Biol. Chem. 294:16740–16755.

Yang, Y., J. Xiong, J. Wang, Y. Ruan, J. Zhang, Y. Tian, J. Wang, L. Liu, Y. Cheng, X. Wang, Y. Xu, J. Wang, M. Yu, B. Zhao, Y. Zhang, H. Li, and R. Jian. 2020. Novel alternative splicing variants of Klf4 display different capacities for self-renewal and pluripotency in mouse embryonic stem cells. Biochem. Biophys. Res. Commun. 532:377–384.

Yeku, O., E. Scotto-Lavino, and M. A. Frohman. 2009. Identification of alternative transcripts using rapid amplification of cDNA ends (RACE). Methods Mol. Biol. 590:279–294.

Yuan, F., W. Hankey, E. J. Wagner, W. Li, and Q. Wang. 2019. Alternative polyadenylation of mRNA and its role in cancer. Gene Dis 8:61–72.

Yue, F., Y. Cheng, A. Breschi, J. Vierstra, W. Wu, T. Ryba, R. Sandstrom, Z. Ma, C. Davis, B. D. Pope, Y. Shen, D. D. Pervouchine, S. Djebali, R. E. Thurman, R. Kaul, E. Rynes, A. Kirilusha, G. K. Marinov, B. A. Williams, D. Trout, H. Amrhein, K. Fisher-Aylor, I. Antoshechkin, G. DeSalvo, L. H. See, M. Fastuca, J. Drenkow, C. Zaleski, A. Dobin, P. Prieto, J. Lagarde, G. Bussotti, A. Tanzer, O. Denas, K. Li, M. A. Bender, M. Zhang, R. Byron, M. T. Groudine, D. McCleary, L. Pham, Z. Ye, S. Kuan, L. Edsall, Y. C. Wu, M. D. Rasmussen, M. S. Bansal, M. Kellis, C. A. Keller, C. S. Morrissey, T. Mishra, D. Jain, N. Dogan, R. S. Harris, P. Cayting, T. Kawli, A. P. Boyle, G. Euskirchen, A. Kundaje, S. Lin, Y. Lin, C. Jansen, V. S. Malladi, M. S. Cline, D. T. Erickson, V. M. Kirkup, K. Learned, C. A. Sloan, K. R. Rosenbloom, B. Lacerda de Sousa, K. Beal, M. Pignatelli, P. Flicek, J. Lian, T. Kahveci, D. Lee, W. J. Kent, M. Ramalho Santos, J. Herrero, C. Notredame, A. Johnson, S. Vong, K. Lee, D. Bates, F. Neri, M. Diegel, T. Canfield, P. J. Sabo, M. S. Wilken, T. A. Reh, E. Giste, A. Shafer, T. Kutyavin, E. Haugen, D. Dunn, A. P. Reynolds, S. Neph, R. Humbert, R. S. Hansen, M. De Bruijn, L. Selleri, A. Rudensky, S. Josefowicz, R. Samstein, E. E. Eichler, S. H. Orkin, D. Levasseur, T. Papayannopoulou, K. H. Chang, A. Skoultchi, S. Gosh, C. Disteche, P. Treuting, Y. Wang, M. J. Weiss, G. A. Blobel, X. Cao, S. Zhong, T. Wang, P. J. Good, R. F. Lowdon, L. B. Adams, X. Q. Zhou, M. J. Pazin, E. A. Feingold, B. Wold, J. Taylor, A. Mortazavi, S. M. Weissman, J. A. Stamatoyannopoulos, M. P. Snyder, R. Guigo, T. R. Gingeras, D. M. Gilbert, R. C. Hardison, M. A. Beer, and B. Ren. 2014. A comparative encyclopedia of DNA elements in the mouse genome. Nature 515:355–364.

Zhao, S., H. Ma, S. Zou, W. Chen, and R. Zhao. 2007. Hepatic lipogenesis in broiler chickens with different fat deposition during embryonic development. J. Vet. Med. A Physiol. Pathol. Clin. Med. 54:1–6.

Zhao, W., D. Blagev, J. L.k. Pollac, and D. J. Erle. 2011. Toward a systematic understanding of mRNA 3′ untranslated regions. Proc. Am. Thorac. Soc. 8:163–166.

Zhao, W., L. Cao, H. Ying, W. Zhang, D. Li, X. Zhu, W. Xue, S. Wu, M. Cao, C. Fu, H. Qi, Y. Hao, Y. C. Tang, J. Qin, T. P. Zhong, X. Lin, L. Yu, X. Li, L. Li, D. Wu, and W. Pan. 2019. Endothelial CDS2 deficiency causes VEGFA-mediated vascular regression and tumor inhibition. Cell Res 29:895–910.